

This is an Open Access document downloaded from ORCA, Cardiff University's institutional repository: <https://orca.cardiff.ac.uk/id/eprint/129392/>

This is the author's version of a work that was submitted to / accepted for publication.

Citation for final published version:

Ellis-Evans, Jennifer and Blenkinsop, Thomas 2019. Analogue modelling of fracturing in cooling plutonic bodies. *Tectonophysics* 766 , pp. 14-19. 10.1016/j.tecto.2019.05.019

Publishers page: <https://doi.org/10.1016/j.tecto.2019.05.019>

Please note:

Changes made as a result of publishing processes such as copy-editing, formatting and page numbers may not be reflected in this version. For the definitive version of this publication, please refer to the published source. You are advised to consult the publisher's version if you wish to cite this paper.

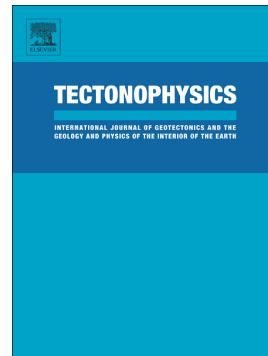
This version is being made available in accordance with publisher policies. See <http://orca.cf.ac.uk/policies.html> for usage policies. Copyright and moral rights for publications made available in ORCA are retained by the copyright holders.



Accepted Manuscript

Analogue modelling of fracturing in cooling plutonic bodies

J.F. Ellis, T. Blenkinsop



PII: S0040-1951(19)30212-4
DOI: <https://doi.org/10.1016/j.tecto.2019.05.019>
Reference: TECTO 128125
To appear in: *Tectonophysics*
Received date: 27 March 2019
Revised date: 23 May 2019
Accepted date: 27 May 2019

Please cite this article as: J.F. Ellis and T. Blenkinsop, Analogue modelling of fracturing in cooling plutonic bodies, *Tectonophysics*, <https://doi.org/10.1016/j.tecto.2019.05.019>

This is a PDF file of an unedited manuscript that has been accepted for publication. As a service to our customers we are providing this early version of the manuscript. The manuscript will undergo copyediting, typesetting, and review of the resulting proof before it is published in its final form. Please note that during the production process errors may be discovered which could affect the content, and all legal disclaimers that apply to the journal pertain.

Analogue modelling of fracturing in cooling plutonic bodies**J. F. Ellis^{a*} and T. Blenkinsop^a***^aSchool of Earth and Ocean Sciences, Cardiff University, Cardiff, CF10 3AT, UK*

*Corresponding author, email address:ellisj11@cardiff.ac.uk

ABSTRACT

Fractures formed when igneous rocks cool below the surface of the Earth are of considerable current interest in studies of hydrology, mineral systems and radioactive waste disposal. However, little is known about the geometry and kinematics of such fractures. Conceptual models suggest that early fractures result from emplacement forces (the Cloos model) while two-dimensional numerical modelling suggests that fractures may result from the contraction of cooling bodies. We use analogue modelling to investigate the geometry of fractures formed in a cylindrical static contracting body. Our experiments show that dehydration of buried starch flour is a workable analogue. Fractures in the analogue material result from drying and contraction of a cylindrical volume which differs from previous experiments in which drying was from a single planar surface and resulted in the formation of columnar joints. In buried analogue models two key fracture sets form internally, producing sub-vertical radial fractures, and concentric fractures that curve downwards with depth. Fracture density decreases towards the centre and bottom of the samples. Samples that were buried more deeply have fewer and less curved concentric fractures than those with shallow burials. Radial fractures have similar orientations to those predicted from numerical models, and concentric fractures are comparable to marginal fissure orientations of the Cloos model. The analogue models suggest that both radial and concentric fractures may result from the contraction of plutonic bodies.

keywords

Analogue modelling, Cooling, Pluton, Fractures

1. Introduction

Fracture sets found within plutonic rocks are the first order control on rock strength, porosity and permeability. These fractures are therefore critical for the formation of ore deposits (e.g. McCaffrey et al., 1999), for understanding rock mass properties required for successful geothermal energy production (e.g. Genter et al., 2010; Villeneuve et al., 2018) and radioactive waste disposal (e.g. Price, 1979; Mariner et al., 2011; Wang et al., 2018). Fractures may result from thermal, tectonic, hydraulic and exhumation-induced stresses, so that the evolution of fracture networks in plutonic rocks may be complex. Earliest fractures are likely to be related to thermal processes and are significant because they may control later fracturing events (Segall and Pollard, 1983; Pollard and Aydin, 1988; Crider, 2015).

The Cloos model is commonly reproduced as a general explanation of early fracture orientations and patterns within plutonic rocks (e.g. Pollard and Aydin, 1988; Price and Cosgrove, 1990; Hills, 1972; Bahat et al., 2005). Fractures are termed cross “joints” (Q), longitudinal “joints” (S), diagonal “joints” (Str), flat lying “joints” and faults (FL) and marginal fissures (T). Fracture orientations are related to flow features represented by foliation and lineation's (Balk, 1937) (Figure 1)¹.

Fracture sets defined in the Cloos model are linked to the mode of emplacement as cooling and crystallisation occurs (Cloos 1922, 1925). For example, cross “joints” and marginal fissures are suggested to result from expansion and arching during pluton emplacement, and diagonal “joints” and flat lying normal faults result from lateral compressive stresses developed during emplacement (Balk, 1937). These mechanisms are likened to fractures forming in wet clays (Riedel 1929; Balk, 1937 p29 plt 12). Although fractures with orientations similar to those of the Cloos model are often observed in the field, their

¹ The term “joint” is given in quotations as these fractures often display evidence of shear movement and may form when the rock is in a plastic state.

relationship to flow lines is controversial (Hutton, 1988; Paterson et al., 1998; Correa-Gomes et al., 2001; Bankwitz et al., 2004; Bahat et al., 2005).

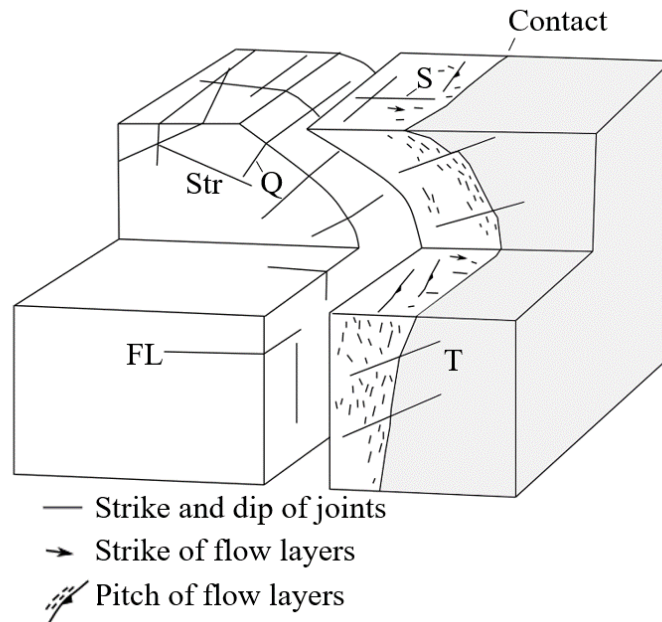


Fig. 1. Block diagram showing the orientation of primary fracture systems within a pluton (white). Q, cross “joints”; S, longitudinal “joints”; FL, flat-lying “joints”; Str, diagonal “joints”; T, marginal fissures. Modified from Hills (1972).

Two-dimensional numerical modelling of fractures in plutonic bodies can predict the stresses as a result of cooling an instantly emplaced hot body in a cooler crust. These models suggest that the formation of early fractures during pluton cooling is controlled by thermal contraction, and fracture orientations are affected by pluton margin geometry, emplacement depth and regional confining loads (Knapp, 1978; Gerla, 1988; Bergbauer et al., 1998; Koenders and Petford, 2003; Žák et al., 2006). In models where the regional load is isotropic, the predicted orientation of the most tensile stress is parallel to the pluton margins, so that tensile fractures are expected to be perpendicular to the margins. For example, in plutons represented by a circle in map view, tensile fractures are predicted to be vertical and radial around the pluton (Bergbauer et al., 1998), Figure 2: tension is defined as positive.

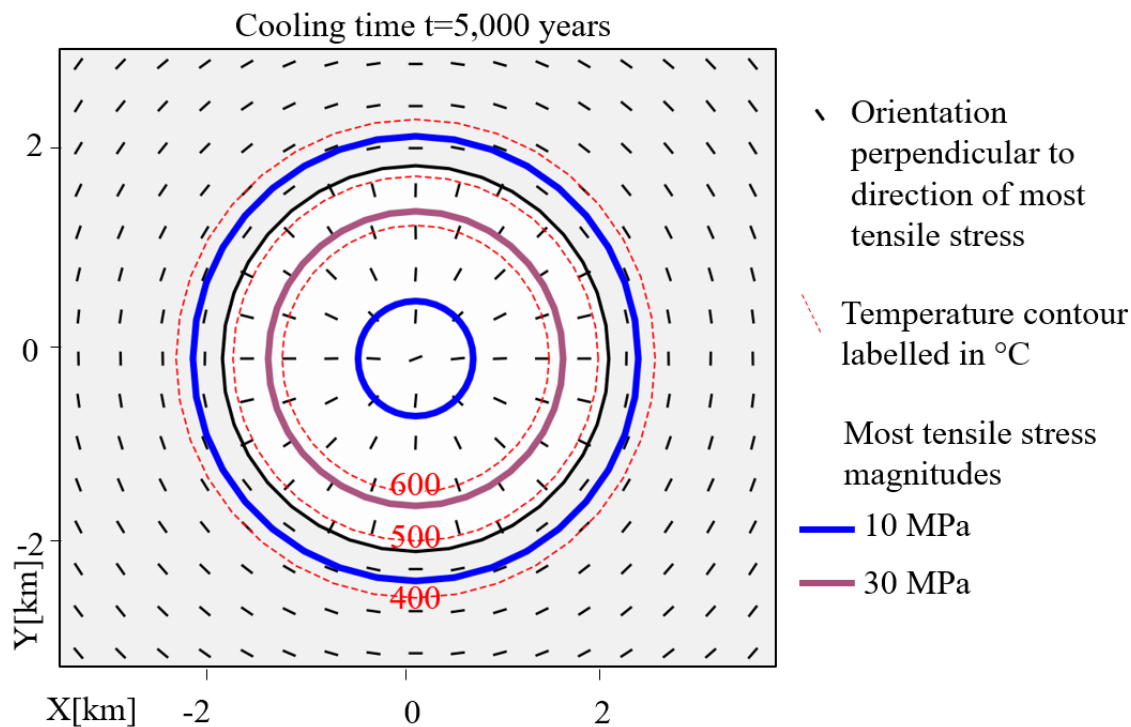


Fig. 2. Numerical model of principal stress orientation and magnitude in a circular intrusion (white) and host rock (grey), after 5,000 years of cooling from start of model run (map view). Black lines are perpendicular to the direction of most tensile stress in the pluton and host rock, coloured contours show magnitudes of most tensile stress, red dashed lines are temperature contours (labelled for temperature in °C). Tension is defined as positive, after Bergbauer et al., (1998).

Previous analogue models of fracturing in plutons have not investigated fracture geometries resulting from the contraction of a volume, the process for early fracture formations suggested by numerical modelling. The aim of the analogue modelling presented in this paper is to determine fracture orientations that could result directly from the contraction of a cylindrical volume. To do this we use drying corn-starch patties. Drying of water saturated corn-starch is analogous to cooling, as both are diffusive processes (Müller, 1998a). Starch experiments have previously been used to give insights into basalt column formation (an end member of fracture patterns resulting from cooling of igneous rocks) (Müller, 1998a, 1998b; Toramaru and Matsumoto, 2004; Goehring et al., 2006) and studies of tensile-crack propagation and crack morphology (Müller and Dahm, 2000; Müller, 2001). In this study we

develop a technique of creating and burying starch patties as an analogue to fracturing in plutons. We test the influence of depth on fracture patterns and geometries in a cylindrical contracting volume. A single cylindrical geometry was chosen to limit the range of variables modelled.

2. Theoretical background

Drying of wet starch results in contraction. Forces resulting from drying of starch exceed the material strength leading to fracture formation (Müller, 1998a,b, 2001). When starch slurries are dried from a single free surface two phases of cracking are identified: initial fracturing at the surface (first-generation cracks) and internal fracturing (second-generation cracks) (Müller, 1998a, 1998b; Toramaru and Matsumoto, 2004; Goehring and Morris, 2005). First-generation cracks are analogous to the formation of fractures in drying mud, forming where the surface tension is eliminated (Müller, 1998a; Goehring 2012; Akiba et al., 2017). Second-generation cracks become more regular. When a critical desiccation rate ($0.8 \times 10^{-5} \text{ g/mm}^2\text{h}$) is exceeded, columnar joints form resulting in polygonal fracture patterns (Müller, 1998a; Toramaru and Matsumoto, 2004).

3. Methodology

Mixtures of 250 g corn-starch (Brown & Polson brand) and 250 ml water (mixed with 1 ~1 tsp of bleach to prevent mould growth, c.f. Goehring and Morris 2005) were prepared. A 1:1 ratio of starch to water was used to fully saturate the starch grains (Müller, 1998b). Acetate moulds were constructed by folding and taping acetate sheets to cylinders, with a 40 mm height and diameter (Figure 3A). The mixture was poured into acetate moulds, Figure 3B) and part dried under a heat lamp to form starch patties (Figure 3C & D).

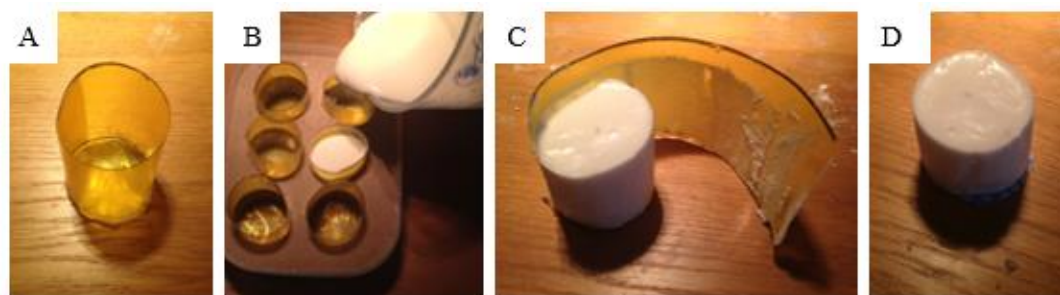


Fig. 3. Recipe for forming corn-starch patties; (A) cylindrical mould formed from taped acetate, 40 mm diameter and height; (B) corn-starch slurry poured into moulds that are placed in sand to maintain shape and prevent leaks; (C) removal of acetate mould once corn-starch patty formed after leaving under heat lamp; (D) example of corn-starch patty prior to burial.

The slurry was dried to the point that it formed a coherent wet mass, before surface cracks formed. This was achieved by placing the mould 50 cm from a 250 W heat lamp (temperature $\sim 30^{\circ}\text{C}$) for 1 hour. The partly dried corn-starch patties can be removed by cutting the tape (Figure 3C).

Various methods of further drying the corn starch patty were then applied. These included drying under the heat lamp with or without the mould, air drying the patty in the mould, or burying the patties removed from the mould. Oven dried sand, corn-starch and calcium chloride desiccant (brand, KontrolKrystals) were used as the burial media to investigate the difference between the influences of drying rate and depth. Burial depths to top of the samples were 5 mm, 10 mm, 20 mm, 40 mm, 60 mm. Three repeats of each sand buried sample were completed to test reproducibility. In the samples where corn-starch and desiccant were used as the burial medium, samples were placed in cloth to help with the removal. A cloth encased sample buried to 20 mm in sand was run as a control for the other burial media.

Drying rate was recorded for selected samples using a mass balance to a precision of two decimal places. The mass of the selected sample was recorded every hour for the first 12 hours of drying and then every 24 hours. Once the weight reduced by $\sim 30\%$ of the original

mass, the samples were broken vertically in half to examine the internal fracture patterns. Lamp dried samples were left for 1 day (no mould) to 6 days (in mould), and air-dried samples were left for 17 days and sand buried samples for a maximum of 6 weeks. The corn-starch buried samples were left for 3 to 12 days depending on burial depth. Desiccant-buried samples were left for a maximum of 5 days.

4. Scaling

The analogue models are scaled to ensure they are geometrically, kinematically and dynamically similar as possible to cooling plutonic bodies (Hubbert 1937; Ramberg 1981; Merle 2015).

A length scaling ratio of 10^{-5} is assumed so that 1 cm in the models is equivalent to 1 km in nature. Shapes of plutons are variable, from thin and extensive tabular bodies, to wedge shaped or cylindrical shaped stocks (e.g. Mendel, 2011), but cylindrical geometries are commonly used as an ideal representation of plutonic bodies (e.g. Pitcher, 1979; Gerla, 1988; Koshmann and Mitchell, 1986; Petford et al., 2000; Annen, 2009; Gelman et al., 2013). The analogue model is comparable to plutonic bodies with a steep sided stock like geometry and volumes $\sim 50 \text{ km}^3$. This geometry is similar, for example, to the cylindrical volume used to model the cooling history of the Alta stock (Cook and Bowman, 1994). Stocks are typically emplaced at shallow-to-mid crustal depth of 1 to 6 km (Menand, 2011), which scale to the analogue burial depths of 10 to 60 mm.

Drying rate is influenced by burial depth and model scaling. The run time of models buried in sand varied between 21 and 39 days. Hydraulic diffusivity of starch (0.01 to $0.03 \text{ mm}^2/\text{s}$) (Müller, 1998a) is ~ 2 to 3 orders of magnitude slower than the thermal diffusivity of basalt (0.9 to $1.2 \text{ mm}^2/\text{s}$) (Müller, 1998a,b; Goehring et al., 2006). Based on this relationship, model run times would scale to natural times of 2,000– 40,000 years. Assuming the three orders of magnitude difference, the scaled model run times are similar to estimates of

solidification time (32,000 years) for a similar sized geometry in numerical models of Knapp and Norton, (1981). This rate may be modified by many other processes not included in numerical models (Knapp, 1978). One of the most significant influences of the thermal evolution is likely to be related to incremental growth history (Glazner et al., 2004; Annen, 2009; Menand, 2011; Annen et al., 2015). Comparable to numerical modelling (Norton and Knight, 1977; Hanson and Glazner, 1995; Bergbauer and Martel, 1999; Zak et al., 2006; Bartley et al., 2008), analogues are representative of a pluton at the point of crystallisation, with an evolutionary history that maintains its temperature prior to cooling as a single unit.

Drying starch-water mixture changes from a liquid with low viscosity to a brittle material with high viscosity and non-zero values of shear modulus and tensile strength (Müller, 1998a). The cohesion of starch ranges from 40 Pa to 260 Pa, depending on water saturation (Stasiak et al., 2013). The analogue material cohesion is therefore $\sim 10^{-6}$ times lower than natural rocks and suitably scaled. The internal friction angle of starch flours (37° ; Stasiak et al., 2013) is comparable to that of rocks ($30^\circ - 40^\circ$; Byerlee 1978). Scaling of the cohesion and internal friction angle is comparable to other analogue experiments, as outlined in Holohan et al., (2008) and Warsitzka et al., (2013). The scaling of brittle material behaviour is theoretically time-independent (Merle, 2015).

5. Results

The geometry of surface and internal fractures varies with burial depth, burial medium and drying method (Figure 3).

5.1. Surface fracture pattern

The fastest dried samples (under the lamp) have the greatest number of surface fractures and form small blocks (~ 0.1 cm – 0.5 cm) with irregular edges (Figure 4i A & B). Air-dried and buried samples form larger surface blocks (~ 0.5 cm to 1 cm), (Figure 4i C & D and Figure 5D to Q). Fracture traces in the buried examples are smoother than in the lamp-dried

examples. Fracture networks on the top surface can be described as random and irregular in lamp dried examples to random and regular in air dried and buried examples (Figure 4i). On the top surface of all samples, fracture trace orientations are perpendicular to the circumference at the periphery, and variable towards the centre of the circle. Fractures extending inwards from the circumference of the top surface are shortest in lamp dried examples (~0.1 cm, Figures 4 and 5. A & B), and increase in length with depth of burial (~ 1 cm at a burial depth of 60cm, Figure 5I). The total trace length of all combined fractures decreases in buried samples as fewer fractures formed. For example, in lamp dried examples the total trace length of all top surface fractures is ~10 cm, whereas in samples buried > 20 mm, the total trace length decreases from ~4 to ~2 cm with depth. Fracture apertures vary between 0.1 and 0.6 mm. A higher proportion of thin apertures are recorded for the surface and shallow buried samples.

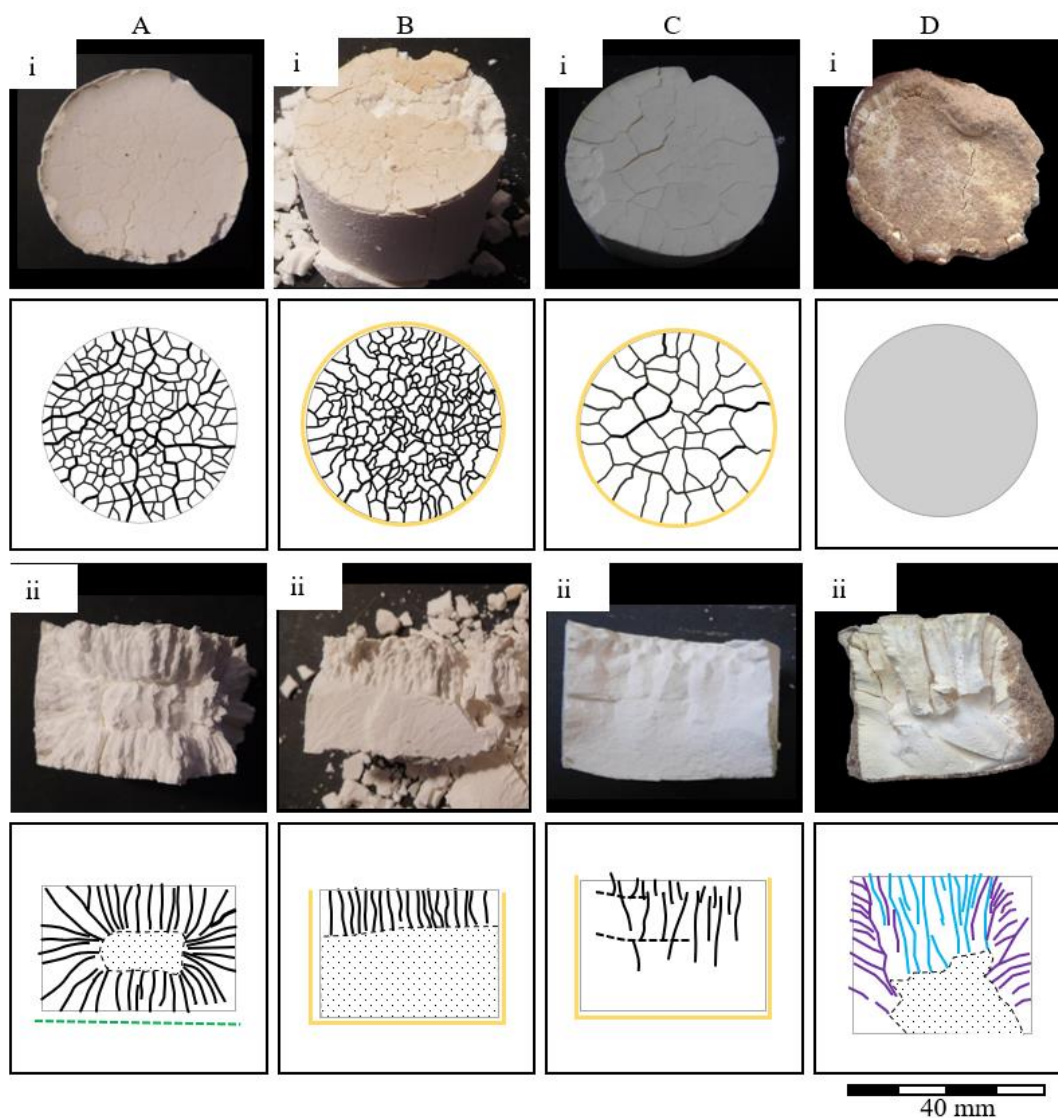


Fig. 4. Comparison of drying methods for cylinders (40 mm diameter by 40 mm height). These samples were generated as starch-patties under the heat lamp before they were left to dry: (A) removed from mould under lamp; (B) left in mould under lamp; (C) air dried in mould; (D) buried in sand with the top of the sample at depth of 5 mm, the surface fracture pattern is obscured by sand. (i) top surface of dried corn-starch patties (ii) broken vertically in half to reveal internal fracture patterns. Internal fracture traces coloured as in Figure 5. Black, traces from polygonal fracture patterns; turquoise, sub-vertical fractures with radial strikes; purple, fractures from vertical margins curve downwards and strike concentrically around the sample. Stippled area; un-fractured domain of damp corn-starch.

5.2. Internal fracture patterns

Internal fractures extend down to a sharp boundary with damp, unfractured corn-starch, marked by a dashed line in Figure 4ii. In the buried samples (i.e. Figure 4ii D) internal

fractures are non-columnar to roughly columnar. Fractures are near vertical and perpendicular to the margins or concentric to the margins and curve downwards.

Lamp dried examples produced smaller (1 mm spacing) and more numerous columns (Figure 4ii A & B) than air-dried examples (~2 to 4 mm spacing) (Figure 4ii C). In both cases the number of fractures decreases with distance from the top of the samples. Fractures formed when the patty is suspended on a cloth form ~1 mm diameter columns perpendicular to every margin of the sample (Figure 4ii B). Fine ~1 mm columns are formed in the desiccant-buried samples. The density of fracturing decreases towards the centre and bottom of each sample. The patties that were buried deeper have fewer and less curved fractures than those with shallow burial (Figure 5). In samples that were cloth covered prior to burial (F, J to Q; Figure 5) fractures formed from the base.

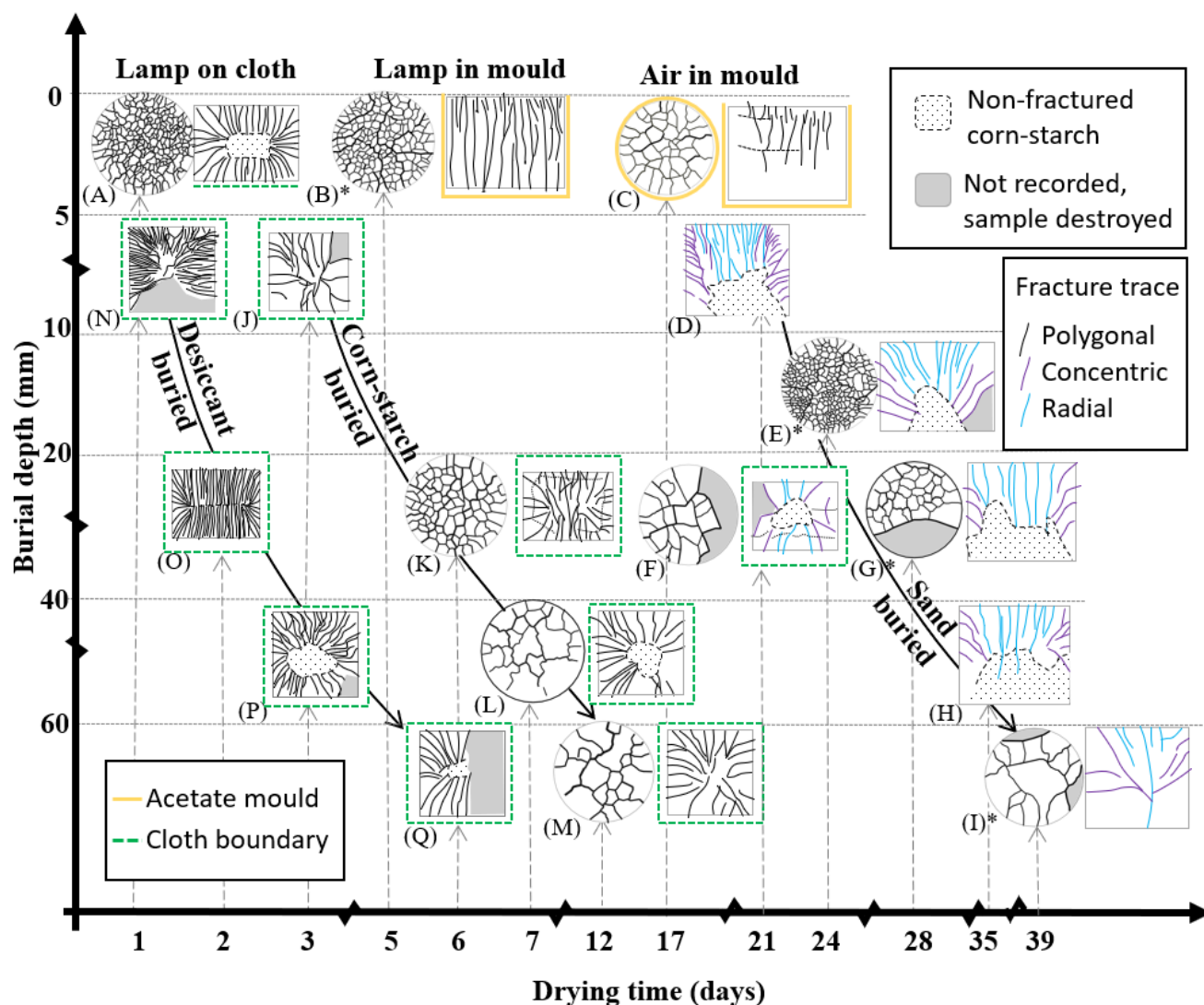


Fig. 5. Sketches for selected fracture patterns presented on a grid of burial depth versus drying rate. Note that scales are not linear. Arrows link drying times (days) to samples. * top and internal patterns from different samples to best represent fracture patterns. Where top circles are not presented, surface patterning was not visible. Surface patterning on the top of the samples is influenced by the drying medium (J to Q). Surface fracture patterns appear more angular in the corn-starch buried example than the sand buried sample without a cloth cover. Sample F was buried in sand with a cloth cover resulting fractures have a similar angular relationship as the other cloth cover samples.

6. Discussion

The trace lengths of fractures extending from the circumference of the top surface are greatest when samples are buried deeper or dried more slowly. Fewer fractures, with smoother traces are formed in the slower dried and deeper buried samples. This may suggest that local

stresses from grain boundaries have less effect with slower desiccation rates, in agreement with Akiba et al., (2017). Internal fracture orientations depend on the surfaces from which drying occurs. Contraction of the volume results in radial and inward dipping fractures, related to radial and vertical tensile forces. The change in dip of concentric fractures indicates a change in stress direction with depth both within the sample and with burial depth (c.f. Odonne and Rolando, 1999). In buried examples covered by cloth, fractures form from the horizontal base of the sample, suggesting that the cloth influences the drying process. The similarity in fracture patterns between repeats of samples buried at the same depth in sand suggests that irregularities, as a result of burial of patties in a semi-solid state, does not affect the results.

6.1. Comparison to conceptual and numerical models

The analogue modelling produces fractures that formed by contraction of drying corn-starch. The radial fracture patterns (Figure 6) mimic fracture orientations predicted by numerical models with circular geometries in map view (Figure 2). The orientation of the concentric fractures in the analogues (Figure 6) are comparable to marginal fissure orientations in the Cloos model (Figure 1). Although the analogue models presented do not rule out the formation of marginal fissures due to emplacement forces, as suggested by Cloos, fractures of a similar orientation may be produced by cooling and contraction. The concentric downward curving fractures (Figure 6) are not predicted in numerical models of cooling. This may be because numerical models have been limited to two-dimensions.

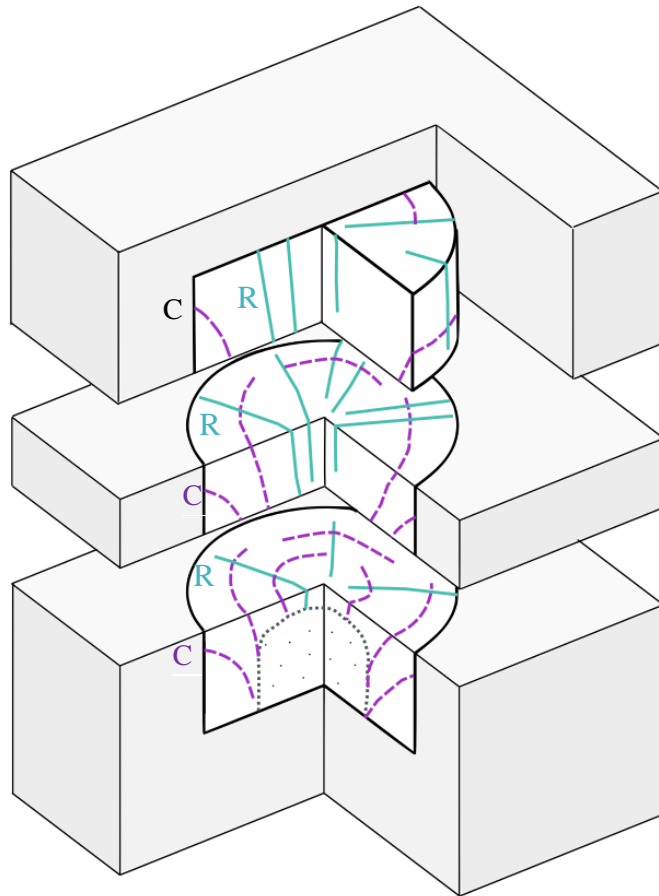


Fig. 6. Sketch of key internal fracture orientations produced in sand buried corn-starch patties R, fractures near vertical with radial strikes; C, fractures from vertical margins, curve downwards and strike concentrically around the sample. Stippled area un-fractured domain of damp corn-starch.

6.2. Comparison to columnar joint formation in drying corn-starch

Columnar joints formed in the samples presented here are not as clearly defined as in published experiments (compare Figure 4 with Müller, 1998b plt 3 & 4). Rates of drying are slower in our samples than previous experiments. The average desiccation rate ($0.3\text{e-}2 \text{ g/cm}^2\text{h}$) calculated for sample C (air dried in mould) and the average desiccation rates ($0.1\text{e-}2 - 0.01\text{e-}2 \text{ g/cm}^2\text{h}$) calculated for the buried samples are lower than the calculated critical desiccation rate for column formation ($0.8\text{e-}2 \text{ g/cm}^2\text{h}$) (Toramaru and Matsumoto, 2004). The

critical desiccation rate for column formation may be lower in our models than in the Toramaru and Matsumoto (2004) experiments because of water retention in the burial media.

7. Conclusions

Corn starch patties, buried to different depths under various media, are potential analogues to plutons cooling at variable depths and rates. For the simple, archetypal cylindrical geometry used here, fracture geometry formed in the analogue samples is controlled by both margin orientation and burial depth of the drying patty. In buried samples, two key fracture orientations are formed: near vertical, perpendicular to the margins, and concentric to the margins, curving downwards. These fracture orientations are comparable to the radial fractures suggested by numerical modelling of cooling, and the marginal fissure orientations of the Cloos model respectively. In contrast to the Cloos model, the analogues suggest that marginal fissure orientations could result from contraction, rather than emplacement forces. Increased burial depth reduces the total number of fractures formed.

Acknowledgements

The experiments presented were performed during Ellis's PhD project under supervision of Thomas Blenkinsop at Cardiff University. Jennifer Ellis PhD is funded by Midland Valley and Cardiff University and supported by Rio Tinto. Hamid Reza Sha Mohammadi is acknowledged for assisting with testing of methods for formation of the corn-starch patties and was funded by CUROP 2017. We thank Jiri Žák and Giulio Viola for their constructive comments which improved this manuscript.

References

Akiba, Y., Magome, J., Kobayashi, H. and Shima, H., 2017. Morphometric analysis of polygonal cracking patterns in desiccated starch slurries. *Physical Review E*, 96(2),

p.023003. <https://doi.org/10.1103/PhysRevE.96.023003>

Annen, C., 2009. From plutons to magma chambers: Thermal constraints on the accumulation of eruptible silicic magma in the upper crust. *Earth and Planetary Science Letters*, 284(3-4), pp.409-416. <https://doi.org/10.1016/j.epsl.2009.05.006>

Letters, 284(3-4), pp.409-416. <https://doi.org/10.1016/j.epsl.2009.05.006>

Annen, C., Blundy, J.D., Leuthold, J. and Sparks, R.S.J., 2015. Construction and evolution of igneous bodies: Towards an integrated perspective of crustal magmatism. *Lithos*, 230, pp.206-221. <https://doi.org/10.1016/j.lithos.2015.05.008>

Bahat, D., Rabinovitch, A. and Frid, V., 2005. Tensile fracturing in rocks.

Tectonofractographic and Electromagnetic Radiation Methods. Springer, Heidelberg. 569pp.

Balk, R. and Cloos, H., 1977. Structural Behavior of Igneous Rocks:(with Special Referenceto Interpretations by H. Cloos and Collaborators) (Vol. 5). Geological Society of America.

Bankwitz, P., Bankwitz, E., Thomas, R., Wemmer, K. and Kämpf, H., 2004. Age and depth evidence for pre-exhumation joints in granite plutons: fracturing during the early cooling stage of felsic rock. *Geological Society, London, Special Publications*, 231(1), pp.25-47. <https://doi.org/10.1144/GSL.SP.2004.231.01.03>

Bartley, J.M., Coleman, D.S. and Glazner, A.F., 2008. Incremental pluton emplacement by magmatic crack-seal. *Earth and Environmental Science Transactions of the Royal Society of Edinburgh*, 97(4), pp.383-396. <https://doi.org/10.1017/S0263593300001528>

Bergbauer, S. and Martel, S.J., 1999. Formation of joints in cooling plutons. *Journal of Structural Geology*, 21(7), pp.821-835. [https://doi.org/10.1016/S0191-8141\(99\)00082-6](https://doi.org/10.1016/S0191-8141(99)00082-6)

Bergbauer, S., Martel, S.J. and Hieronymus, C.F., 1998. Thermal stress evolution in cooling pluton environments of different geometries. *Geophysical Research Letters*, 25(5), pp.707-710. <https://doi.org/10.1029/98GL00047>

Byerlee, J., 1978. Friction of rocks. In *Rock friction and earthquake prediction* (pp. 615-626).

Birkhäuser, Basel.

Cook, S.J. and Bowman, J.R., 1994. Contact metamorphism surrounding the Alta stock:

Thermal constraints and evidence of advective heat transport from calcite+ dolomite geothermometry. *American Mineralogist*, 79(5-6), pp.513-525.

Correa-Gomes, L.C., Souza Filho, C.R., Martins, C.J.F.N. and Oliveira, E.P., 2001.

Development of symmetrical and asymmetrical fabrics in sheet-like igneous bodies: the role of magma flow and wall-rock displacements in theoretical and natural cases. *Journal of Structural Geology*, 23(9), pp.1415-1428.

[https://doi.org/10.1016/S0191-8141\(01\)00007-4](https://doi.org/10.1016/S0191-8141(01)00007-4)

Cloos, H., 1922. *Der Gebirgsbau Schlesiens und die Stellung seiner Bodenschätze*. Verlag von

Gebrüder Borntraeger.

Cloos, H., 1925. *Das Riesengebirge in Schlesien. Einführung in die tektonische Behandlung*

magmatischer Erscheinungen.

Crider, J.G., 2015. The initiation of brittle faults in crystalline rock. *Journal of Structural*

Geology, 77, pp.159-174. <https://doi.org/10.1016/j.jsg.2015.05.001>

Gelman, S.E., Gutiérrez, F.J. and Bachmann, O., 2013. On the longevity of large upper

crustal silicic magma reservoirs. *Geology*, 41(7), pp.759-762.

<https://doi.org/10.1130/G34241.1>

Genter, A., Evans, K., Cuenot, N., Fritsch, D. and Sanjuan, B., 2010. Contribution of the

exploration of deep crystalline fractured reservoir of Soultz to the knowledge of

enhanced geothermal systems (EGS). *Comptes Rendus Geoscience*, 342(7-8), pp.502-

516. <https://doi.org/10.1016/j.crte.2010.01.006>

Gerla, P.J., 1988. Stress and fracture evolution in a cooling pluton: An example from the

Diamond Joe stock, western Arizona, USA. *Journal of Volcanology and Geothermal*

- Research, 34(3-4), pp.267-282. [https://doi.org/10.1016/0377-0273\(88\)90038-8](https://doi.org/10.1016/0377-0273(88)90038-8)
- Glazner, A.F., Bartley, J.M., Coleman, D.S., Gray, W. and Taylor, R.Z., 2004. Are plutons assembled over millions of years by amalgamation from small magma chambers?. *GSA today*, 14(4/5), pp.4-12. [https://doi.org/10.1130/1052-5173\(2004\)014<0004](https://doi.org/10.1130/1052-5173(2004)014<0004)
- Goehring, L., Morris, S.W. and Lin, Z., 2006. Experimental investigation of the scaling of columnar joints. *Physical Review E*, 74(3), p.036115. <https://doi.org/10.1103/PhysRevE.74.036115>
- Goehring, L., 2013. Evolving fracture patterns: columnar joints, mud cracks and polygonal terrain. *Philosophical Transactions of the Royal Society A: Mathematical, Physical and Engineering Sciences*, 371(2004), p.20120353. <https://doi.org/10.1098/rsta.2012.0353>
- Hills, E.S., 1972. *Elements of Structural Geology*. Springer Netherlands. <https://doi.org/10.1007/978-94-009-5843-2>
- Brooks Hanson, R. and Glazner, A.F., 1995. Thermal requirements for extensional emplacement of granitoids. *Geology*, 23(3), pp.213-216. [https://doi.org/10.1130/0091-7613\(1995\)023<0213:TRFEEO>2.3.CO;2](https://doi.org/10.1130/0091-7613(1995)023<0213:TRFEEO>2.3.CO;2)
- Holohan, E.P., de Vries, B.V.W. and Troll, V.R., 2008. Analogue models of caldera collapse in strike-slip tectonic regimes. *Bulletin of Volcanology*, 70(7), pp.773-796. <https://doi.org/10.1007/s00445-007-0166-x>
- Hubbert, M.K., 1937. Theory of scale models as applied to the study of geologic structures. *Bulletin of the Geological Society of America*, 48(10), pp.1459-1520. <https://doi.org/10.1130/GSAB-48-1459>
- Hutton, D.H., 1988. Granite emplacement mechanisms and tectonic controls: inferences from deformation studies. *Earth and Environmental Science Transactions of the Royal Society of Edinburgh*, 79(2-3), pp.245-255. <https://doi.org/10.1017/S0263593300014255>
- Knapp, R.B., 1978. Consequences of heat dispersal from hot plutons [Ph.D. thesis]. The

University of Arizona.

- Knapp, R.B. and Norton, D., 1981. Preliminary numerical analysis of processes related to magma crystallization and stress evolution in cooling pluton environments. *American Journal of Science*, 281(1), pp.35-68. <https://doi.org/10.2475/ajs.281.1.35>
- Koenders, M.A. and Petford, N., 2003. Thermally induced primary fracture development in tabular granitic plutons: a preliminary analysis. *Geological Society, London, Special Publications*, 214(1), pp.143-150. <https://doi.org/10.1144/GSL.SP.2003.214.01.09>
- Kohsmann, J.J. and Mitchell, B.J., 1986. Transient thermoelastic stresses produced by a buried cylindrical intrusion. *Journal of volcanology and geothermal research*, 27(3-4), pp.323-348. [https://doi.org/10.1016/0377-0273\(86\)90019-3](https://doi.org/10.1016/0377-0273(86)90019-3)
- Mariner, P.E., Lee, J.H., Hardin, E.L., Hansen, F.D., Freeze, G.A., Lord, A.S., Goldstein, B. and Price, R.H., 2011. Granite disposal of US high-level radioactive waste. Sandia National Laboratories Scientific Report SAND2011-6203. Albuquerque, New Mexico.
- McCaffrey, K.J.W., Sleight, J.M., Pugliese, S. and Holdsworth, R.E., 2003. Fracture formation and evolution in crystalline rocks: Insights from attribute analysis. *Geological Society, London, Special Publications*, 214(1), pp.109-124. <https://doi.org/10.1144/GSL.SP.2003.214.01.07>
- Menand, T., 2011. Physical controls and depth of emplacement of igneous bodies: A review. *Tectonophysics*, 500(1-4), pp.11-19. <https://doi.org/10.1016/j.tecto.2009.10.016>
- Merle, O., 2015. The scaling of experiments on volcanic systems. *Frontiers in Earth Science*, 3, p.26. <https://doi.org/10.3389/feart.2015.00026>
- Müller, G., 2001. Experimental simulation of joint morphology. *Journal of Structural Geology*, 23(1), pp.45-49. [https://doi.org/10.1016/S0191-8141\(00\)00104-8](https://doi.org/10.1016/S0191-8141(00)00104-8)
- Müller, G., 1998a. Experimental simulation of basalt columns. *Journal of Volcanology and Geothermal Research*, 86(1-4), pp.93-96. [https://doi.org/10.1016/S0377-0273\(98\)00045-](https://doi.org/10.1016/S0377-0273(98)00045-)

- Müller, G., 1998b. Starch columns: Analog model for basalt columns. *Journal of Geophysical Research: Solid Earth*, 103(B7), pp.15239-15253. <https://doi.org/10.1029/98JB00389>
- Müller, G. and Dahm, T., 2000. Fracture morphology of tensile cracks and rupture velocity. *Journal of Geophysical Research: Solid Earth*, 105(B1), pp.723-738. <https://doi.org/10.1029/1999JB900314>
- Norton, D. and Knight, J., 1977. Transport phenomena in hydrothermal systems: cooling plutons. *Am. J. Sci.:(United States)*, 277. <https://doi.org/10.2475/ajs.277.8.937>
- Odonne, F., Ménard, I., Massonnat, G.J. and Rolando, J.P., 1999. Abnormal reverse faulting above a depleting reservoir. *Geology*, 27(2), pp.111-114. [https://doi.org/10.1130/0091-7613\(1999\)027<0111:ARFAAD>2.3.CO;2](https://doi.org/10.1130/0091-7613(1999)027<0111:ARFAAD>2.3.CO;2)
- Paterson, S.R., Fowler Jr, T.K., Schmidt, K.L., Yoshinobu, A.S., Yuan, E.S. and Miller, R.B., 1998. Interpreting magmatic fabric patterns in plutons. *Lithos*, 44(1-2), pp.53-82. [https://doi.org/10.1016/S0024-4937\(98\)00022-X](https://doi.org/10.1016/S0024-4937(98)00022-X)
- Petford, N., Cruden, A.R., McCaffrey, K.J.W. and Vigneresse, J.L., 2000. Granite magma formation, transport and emplacement in the Earth's crust. *Nature*, 408(6813), p.669. <https://doi.org/10.1038/35047000>
- Pitcher, W.S., 1979. The nature, ascent and emplacement of granitic magmas. *Journal of the Geological Society*, 136(6), pp.627-662. <https://doi.org/10.1144/gsjgs.136.6.0627>
- Pollard, D.D. and Aydin, A., 1988. Progress in understanding jointing over the past century. *Geological Society of America Bulletin*, 100(8), pp.1181-1204. [https://doi.org/10.1130/0016-7606\(1988\)100<1181](https://doi.org/10.1130/0016-7606(1988)100<1181)
- Price, N.J., 1979. Fracture patterns and stresses in granites. *Geoscience Canada*, 6(4).
- Price, N.J. and Cosgrove, J.W., 1990. *Analysis of geological structures*. Cambridge University Press.

- Ramberg, H., 1981. The role of gravity in orogenic belts. Geological Society, London, Special Publications, 9(1), pp.125-140. <https://doi.org/10.1144/GSL.SP.1981.009.01.11>
- Riedel, W., 1929. Zur Mechanik geologischer Brucherscheinungen ein Beitrag zum Problem den Fiederpatten. Cent. Blatt Mineral. Geol. Paläont., pp.354-368.
- Segall, P. and Pollard, D.D., 1983. Nucleation and growth of strike slip faults in granite. *Journal of Geophysical Research: Solid Earth*, 88(B1), pp.555-568. <https://doi.org/10.1029/JB088iB01p00555>
- Stasiak, M., Molenda, M., Opaliński, I. and Błaszczak, W., 2013. Mechanical properties of native maize, wheat, and potato starches. *Czech Journal of Food Sciences*, 31(4), pp.347-354.
- Toramaru, A. and Matsumoto, T., 2004. Columnar joint morphology and cooling rate: A starch- water mixture experiment. *Journal of Geophysical Research: Solid Earth*, 109(B2). <https://doi.org/10.1029/2003JB002686>
- Villeneuve, M.C., Heap, M.J., Kushnir, A.R., Qin, T., Baud, P., Zhou, G. and Xu, T., 2018. Estimating in situ rock mass strength and elastic modulus of granite from the Soultz-sous-Forêts geothermal reservoir (France). *Geothermal Energy*, 6(1), p.11. <https://doi.org/10.1186/s40517-018-0096-1>
- Wang, J., Chen, L., Su, R. and Zhao, X., 2018. The Beishan underground research laboratory for geological disposal of high-level radioactive waste in China: Planning, site selection, site characterization and in situ tests. *Journal of Rock Mechanics and Geotechnical Engineering*, 10(3), pp.411-435. <https://doi.org/10.1016/j.jrmge.2018.03.002>
- Warsitzka, M., Kley, J. and Kukowski, N., 2013. Salt diapirism driven by differential loading—Some insights from analogue modelling. *Tectonophysics*, 591, pp.83-97. <https://doi.org/10.1016/j.tecto.2011.11.018>
- Žák, J., Vyhánek, B. and Kabele, P., 2006. Is there a relationship between magmatic fabrics

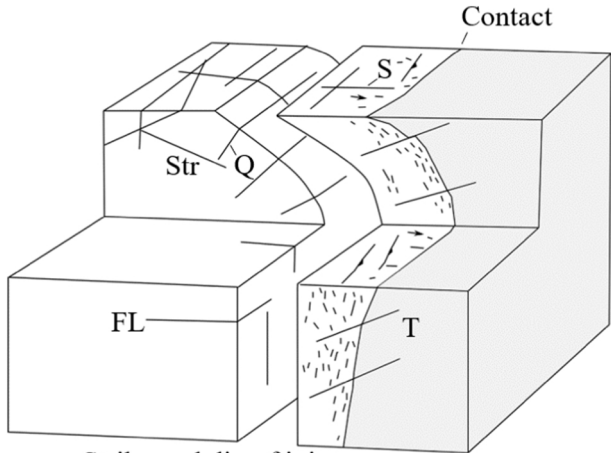
and brittle fractures in plutons? A view based on structural analysis, anisotropy of magnetic susceptibility and thermo-mechanical modelling of the Tanvald pluton (Bohemian Massif). *Physics of the Earth and Planetary Interiors*, 157(3-4), pp.286-310.
<https://doi.org/10.1016/j.pepi.2006.05.001>

ACCEPTED MANUSCRIPT

Highlights

- Analogue models to understand fracturing of plutons during cooling.
- Radial and concentric, steepening downwards, fractures are formed in contracting cylindrical volumes.
- Results depend on rate of contraction and burial depth.

ACCEPTED MANUSCRIPT



- Strike and dip of joints
- Strike of flow layers
- ↗ Pitch of flow layers

Figure 1

Cooling time $t=5,000$ years

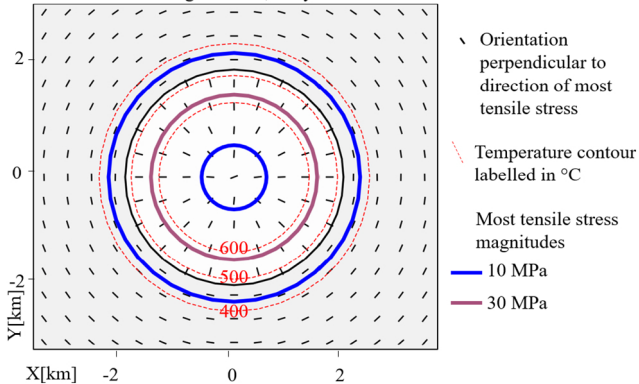
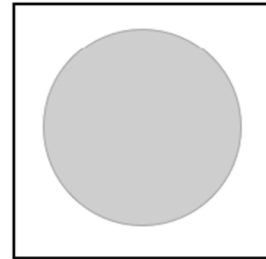
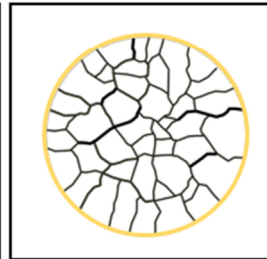
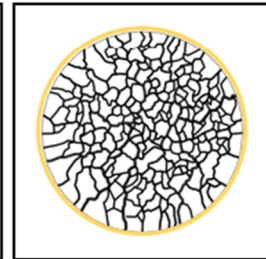
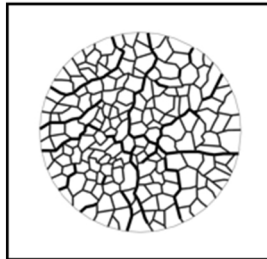
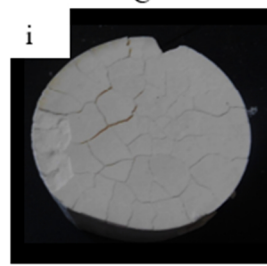
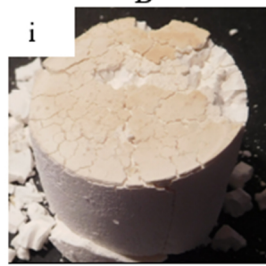
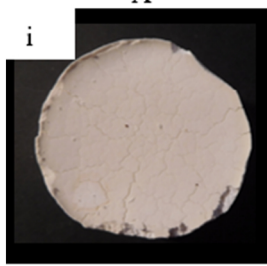
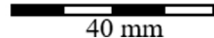
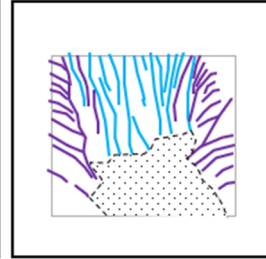
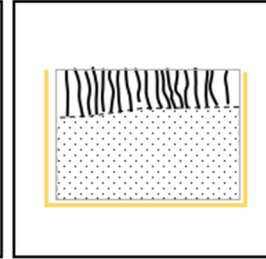
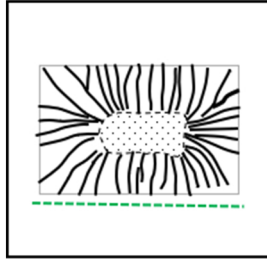
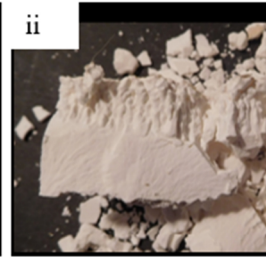


Figure 2



Figure 3

A**B****C****D****i****i****i****i****ii****ii****ii****ii**

40 mm

Figure 4

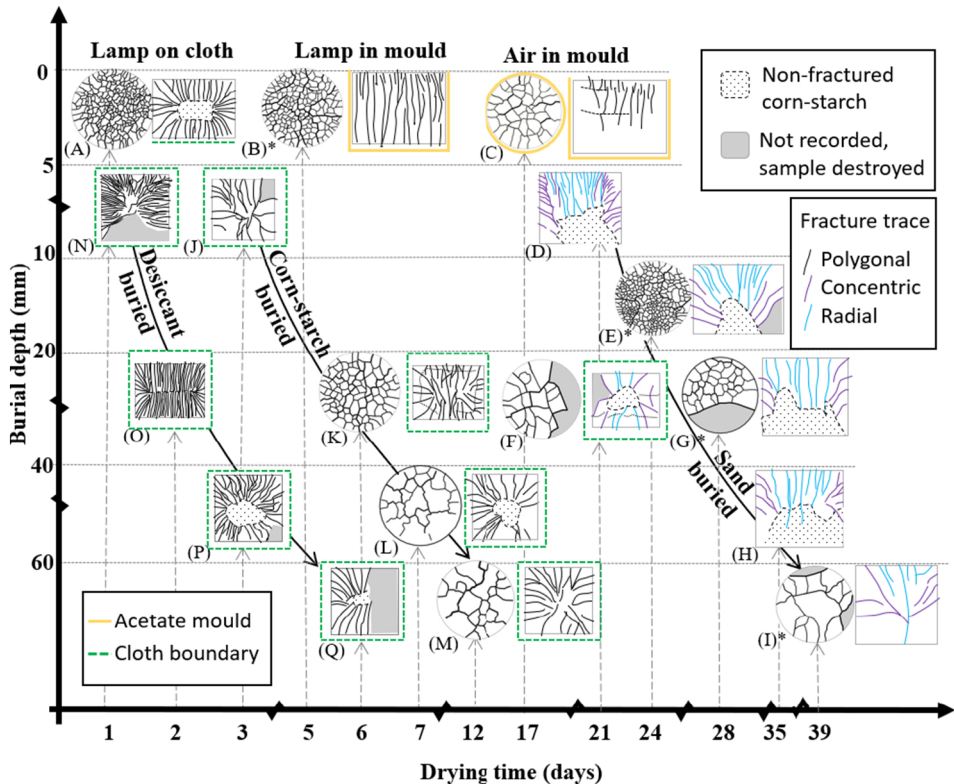


Figure 5

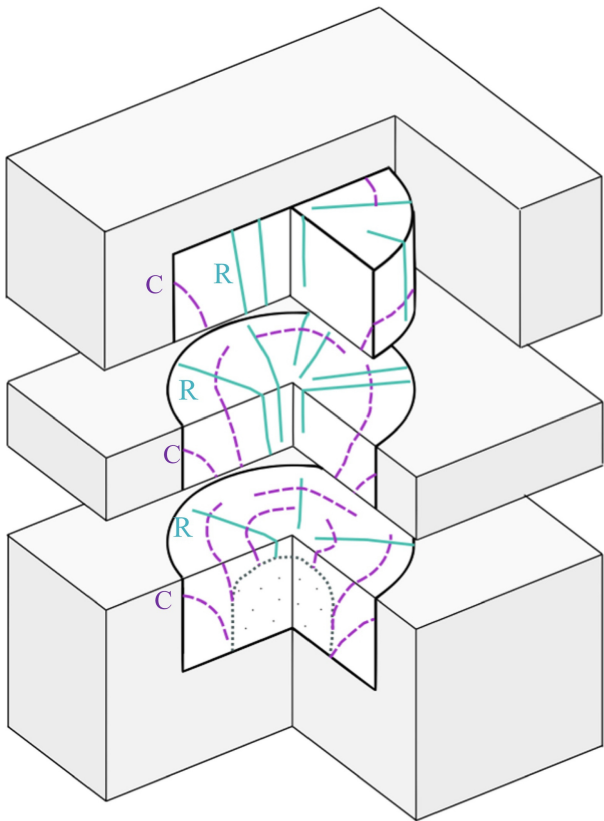


Figure 6